EurJIC European Journal of Inorganic Chemistry
ChemPubSoc Europe
SHORT COMMUNICATION

DOI:10.1002/ejic.201300909

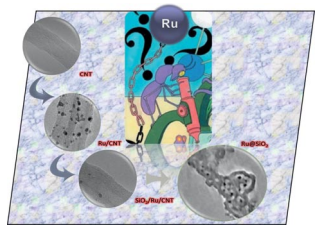

COVER PICTURE

Selective Confinement of Ruthenium Nanoparticles in Silica Nanotubes

T. Trang Nguyen,[a] Ovidiu Ersen,[b] and Philippe Serp*[a]

Keywords: Confinement / Nanoparticles / Nanotubes / Ruthenium / Silica

One hundred percent confinement of ruthenium nanoparticles inside silica nanotubes was reached for the first time in bulk by a simple synthesis strategy involving the use of carbon nanotubes as template.

Introduction

The possibility to perform chemistry in nanoreactors, in which the different phases are subject to confinement effects, has recently attracted great interest from the scientific community.[1] The modified behavior of the confined phase, including transport, adsorption, phase transitions, diffusion, and structure, might directly affect the course of chemical reactions, including hydrogen storage.[2] In the case of supported catalysts, metal nanoparticles (NPs) can be entrapped and stabilized within well-defined pores to prevent aggregation. The orientation and configuration of metal NPs can also be modified as a result of spatial restriction, which could directly influence their catalytic activity through interaction with reactants, intermediates, and/or products. In addition to zeolites,[3] aluminosilicates,[3a] mesoporous silicates,[4] and carbon nanotubes (CNTs),[1a,1b,5] silica nanotubes (SiO_2NTs) represent a new type of material with a well-defined pore structure.[6] Different strategies have been proposed to fill CNTs with metal NPs, including two-step biphasic impregnation,[7] impregnation and selective washing,[8] and molecular recognition.[9] However, none of these approaches allow 100% selectivity to be reached in the confinement, particularly for nanotubes with small internal diameters (<15 nm), which is very important to accurately determine confinement effects. Currently, the definition of efficient techniques for filling small nanotubes at the bulk scale is still a synthesis challenge. As far as SiO_2NTs are concerned, no selective approach for NP confinement has been reported up to now. A few studies have been reported with the use of metal-supported SiO_2NT catalysts. Pt/CNTs were covered with silica layers by hydrolysis of 3-aminopropyltriethoxysilane and/or tetraethoxysilane (TEOS). The silica-coated Pt/CNT showed high catalytic activity for electrochemical reactions in aqueous H_2SO_4 electrolyte, despite the uniform coverage of the Pt metal with silica layers.[10] Pt/CNT[11] and PtAu/CNT[12] catalysts were covered by a porous SiO_2 layer to improve their thermal and electrochemical stability. SiO_2NTs were synthesized with CNTs as the template and used as a support to prepare a ruthenium-based catalyst by a slurry impregnation method. The Ru NPs were mainly located inside the SiO_2NTs. Compared to Ru/SiO_2, the Ru/SiO_2NT catalyst exhibits higher activity for Fischer–Tropsch synthesis.[13] Similar results were reported for Co/SiO_2NT catalysts.[14]

In the present communication, we report a simple method for the ultraselective confinement of Ru NPs inside SiO_2NTs. To the best of our knowledge, no example has been reported for the 100% confinement of NPs in nanotubes. The synthetic strategy is outlined in Scheme 1. It consists of: (1) the preparation of a Ru/CNT by wet impregnation from a ruthenium precursor, (2) the deposition of a silica coating on the Ru/CNT by hydrolysis of TEOS to produce SiO_2/Ru/CNT, and (3) a calcination step in air to burn the CNT template, followed by reduction of the Ru NPs to produce Ru@SiO_2NT.

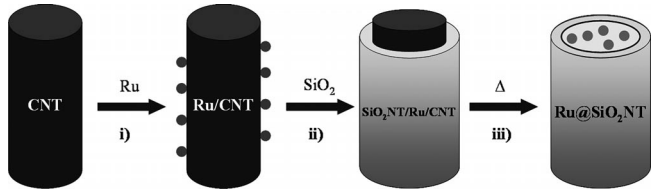

Scheme 1. Synthetic route for the production of ruthenium NPs confined in SiO_2NTs.

[a] Laboratoire de Chimie de Coordination UPR CNRS 8241, composante ENSIACET, Université de Toulouse UPS-INP-LCC
4 allée Emile Monso, BP 44362, 31030 Toulouse Cedex 4, France
E-mail: philippe.serp@ensiacet.fr
http://www.lcc-toulouse.fr/lcc/spip.php?article265
[b] IPCMS – Groupe Surfaces et Interfaces, CNRS – ULP UMR 7504,
23 Rue du Loess, BP 43, 67034 Strasbourg, France

Supporting information for this article is available on the WWW under http://dx.doi.org/10.1002/ejic.201300909

Results and Discussion

Given that a hydrophilic CNT surface is desirable for good adherence of the SiO_2 coating, we used nitric acid oxidized multiwalled CNTs (S_{BET} = 271 $m^2 g^{-1}$; external diameter: 12.3 nm). HNO_3 oxidation involved the initial rapid formation of carbonyl groups, which were consecutively transformed into phenol and carboxylic groups.[15] HNO_3 oxidation also increased the BET surface area and pore volume as a result of CNT tip opening. The use of CNTs as a template for the growth of SiO_2NTs has already been reported. SiO_2NTs have been produced (1) by grafting 2-aminoethyl 3-aminopropyltrimethoxysilane on oxidized CNTs,[16] (2) by treating acyl chloride functionalized CNTs with 3-aminopropyltriethoxysilane,[17] (3) by hydrolysis of TEOS by using polyethylene glycol functionalized CNTs,[18] and (4) by a facile sol–gel process involving acid-oxidized CNTs and hydrolysis of TEOS.[19]

In a first step, we validated that SiO_2NTs were effectively produced by TEOS hydrolysis on the oxidized CNT template without Ru NPs on its surface. The as-produced SiO_2NTs were characterized by TEM (Figure 1), nitrogen adsorption, and thermogravimetric analysis (TGA; Figure S1, Supporting Information). The internal diameter and wall thickness of the SiO_2NTs are in the 9–15 nm and 10–12 nm ranges, respectively. The specific surface area of the SiO_2NTs is 129 $m^2 g^{-1}$; the porous volume is 0.59 $cm^3 g^{-1}$ and the majority of the pores range between 2 and 9 nm.

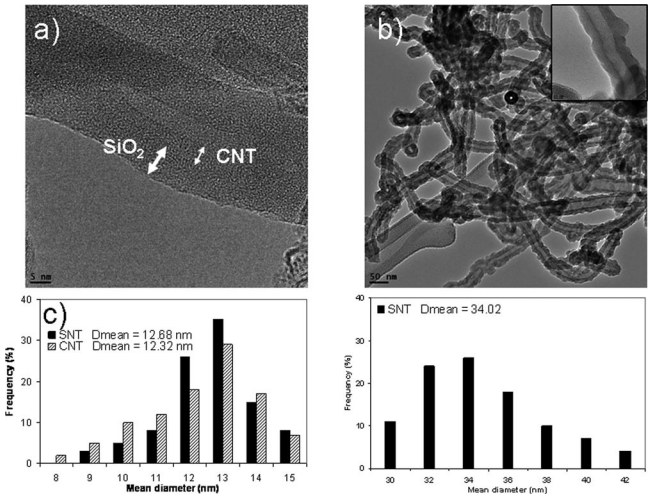

Figure 1. TEM micrographs of (a) SiO_2NT/CNT, (b) SiO_2NT, and (c) internal and external diameters of SiO_2NT.

In a second step, we checked that our approach led to better selectivity for confinement than that already reported for the slurry impregnation method.[13] Ruthenium-supported catalysts were prepared from [$Ru_3(CO)_{12}$] on oxidized CNTs or on preformed SiO_2NTs. The sample prepared from the slurry impregnation method (reduction temperature 300 °C), named Ru1/SiO_2NT, presented 75% of the Ru NPs inside the SiO_2NTs (Figure 2a). The Ru1@SiO_2NT sample, prepared by using CNTs as a template (calcination at 650 °C, followed by reduction at 300 °C), showed a filling yield of 100% (Figure 2b). Metal loadings, NP size, and filling yields are reported in Table 1.

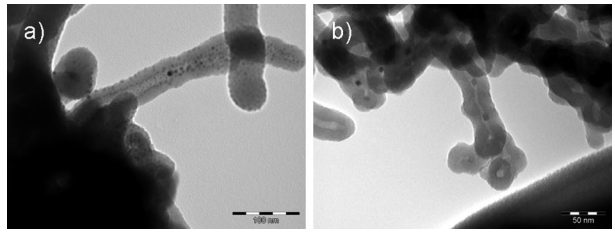

Figure 2. TEM micrographs of (a) Ru1/SiO_2NT and (b) Ru1@SiO_2NT.

Table 1. Metal loading, NP size, and filling yield of the prepared materials.

Sample	Ru loading (% w/w)	NP size (nm)[a]	NP size (nm)[b]	Filling yield (%)
Ru1/SiO_2NT	2.43	3.5	–	75
Ru1/CNT	2.83	3.8	–	40
Ru1@SiO_2NT	1.17	5.5	6.7	100
Ru2/CNT	1.90	1.4	–	58
Ru2@SiO_2NT	0.37	4.8	5.6	100
Ru3/CNT	1.30	1.1	–	52
Ru3@SiO_2NT	0.24	2.5	1.9 ± 0.6	95

[a] From TEM. [b] From XRD.

For Ru1/SiO_2NT, the mean particle size ranged between 2 and 6 nm (mean diameter 3.5 nm), and most of the NPs were spherical, whereas for Ru1@SiO_2NT, the mean particle size ranged between 5 and 8 nm with a mean diameter of 5.5 nm (compared to 2–8 nm, mean diameter 3.8 nm for the Ru1/CNT sample), and most of the NPs were faceted. The presence of faceted nanoparticles on the Ru1@SiO_2NT sample should arise from a strong metal–support interaction on the CNT support. The formation of faceted Ru nanoparticles on the CNT surface has already been reported.[20] The larger particle size obtained for the Ru1@SiO_2NT sample should also arise from the nature of the support, SiO_2 versus CNTs, and from the high-temperature calcination treatment. No severe aggregation of the NPs was noticed, as was reported for Pt NPs.[10,21] XRD analyses confirmed the presence of metallic ruthenium for both reduced samples. The lower Ru loading obtained for Ru1@SiO_2NT relative to that obtained for Ru1/CNT should be correlated to the fact that 40% of the Ru NPs of Ru1/CNT are confined in the inner cavity of the CNTs. We believe that these particles do not anchor on the SiO_2NT surface during the calcination step.

In a third step, given that the nature of the CNT/SiO_2NT interface should play a role in silica grafting, we studied the influence of the dispersion of the Ru NPs on the structure of the final material. Three 3%Ru/CNT samples were prepared on oxidized CNTs by wet impregnation, from three different Ru precursors, [$Ru_3(CO)_{12}$] (Ru1/CNT), $RuCl_3$ (Ru2/CNT), and [Ru(cod)(cot)] (Ru3/CNT; cod = 1,5-cyclooctadiene, cot = 1,3,5-cyclooctatriene). After reduction,

the mean particle size (Figure S2, Supporting Information) ranged between 2 and 6 nm for Ru1/CNT (mean diameter 3.8 nm, 40% of confined Ru NPs), 1 and 3 nm for Ru2/CNT (mean diameter 1.4 nm, 53% of confined Ru NPs), and <1.1 nm for Ru3/CNT (52% of confined Ru NPs). After silica deposition, the thickness of the SiO_2 coating was 10–12 nm for SiO_2NT/Ru1/CNT with a homogeneous coating (Figure S2, Supporting Information). If the Ru dispersion was increased, as for Ru2/CNT, the silica coating of SiO_2NT/Ru2/CNT was still homogeneous, but its thickness decreased to 6–9 nm (Figure S3, Supporting Information). Finally, in the case of SiO_2NT/Ru3/CNT, the measured SiO_2 thickness ranged between 6 and 9 nm, but we occasionally noticed a non-homogeneous coating (Figure S3, Supporting Information). This phenomenon could be due to the presence of a higher density of small Ru clusters on the CNT surface that hinders the SiO_2-shell–oxidized-CNT interaction. Accordingly, a decrease in the C–O–Si bonds in favor of the Ru–O–C bonds reduces the efficiency of silica coating. After the calcination step at 650 °C to remove the CNT template, all of the ruthenium was present as RuO_2 (Figure S4, Supporting Information), as verified by XRD of the three Rux@SiO_2NT samples. Notably, such high-temperature calcination may induce SiO_2 segregation to the surface of RuO_2, which results in the formation of SiO_2 patches.[22] The XRD patterns of the three Rux@SiO_2NT reduced samples (reduction temperature 350 °C) show peaks at $2\theta \approx 22.5°$ (large) that correspond to SiO_2NTs and reflections at 38.7, 42.5, 44.2, 58.6, and 69.8° that correspond to the (100), (002), (101), (102), and (110) planes of metallic ruthenium, respectively, and these data are consistent with a hexagonal crystal structure and establish the presence of Ru^0 (Figure S4, Supporting Information). Trace amounts of RuO_2 were also detected in the three samples. This might be due to (1) air autocatalytic oxidation of the smaller Ru NPs,[23] (2) SiO_2-induced modification of the surface of the RuO_2 NPs,[22] or (3) a strong Ru–SiO_2 interaction.[24] The Rux@SiO_2NT samples were observed by TEM to evaluate the confinement efficiency. These TEM observations revealed another effect of Ru dispersion. As the Ru dispersion increased inside the Rux@SiO_2NT, TEM observation under the electron beam was almost impossible, as most of the Ru2@SiO_2NT samples, and particularly the Ru3@SiO_2NT samples, were damaged under irradiation. Indeed, the presence of numerous small NPs in the SiO_2NT induced the immediate collapse of the SiO_2 structure under irradiation to produce Ru NPs encapsulated inside SiO_2 nanowires (Figure S5, Supporting Information). The formation of such core–shell structures, which can function as microcapsular-like reactors, can also be of interest for catalysis applications.[25] Therefore, to evaluate the confinement efficiency, we performed 2D and 3D cryo-TEM observations (Figure 3). The dispersion of the three samples followed the order Ru3@SiO_2NT > Ru2@SiO_2NT ≈ Ru1@SiO_2NT. The measured Ru particle size ranged from 5 to 8 nm for the Ru1@SiO_2NT (6.7 nm from XRD) and Ru2@SiO_2NT (5.6 nm from XRD) samples and from 1.5 to 2.5 nm for Ru3@SiO_2NT with few a particles at 4–5 nm (1.9 nm from XRD). For the Ru1@SiO_2NT and Ru2@SiO_2NT samples, 100% of the nanoparticles were confined inside the silica nanotubes. For the Ru3@SiO_2NT sample, a few (<5%) small-diameter particles were also observed on the external walls of the SiO_2NTs. The presence of Ru NPs on the external surface of the SiO_2NTs could be due to diffusion/migration of small Ru/RuO_2 clusters during the calcination step. There also, the lower loading obtained for the SiO_2NT-confined Ru NPs related to the Ru/CNT samples should find its origin in the percentage of Ru NPs confined in the Ru/CNT samples.

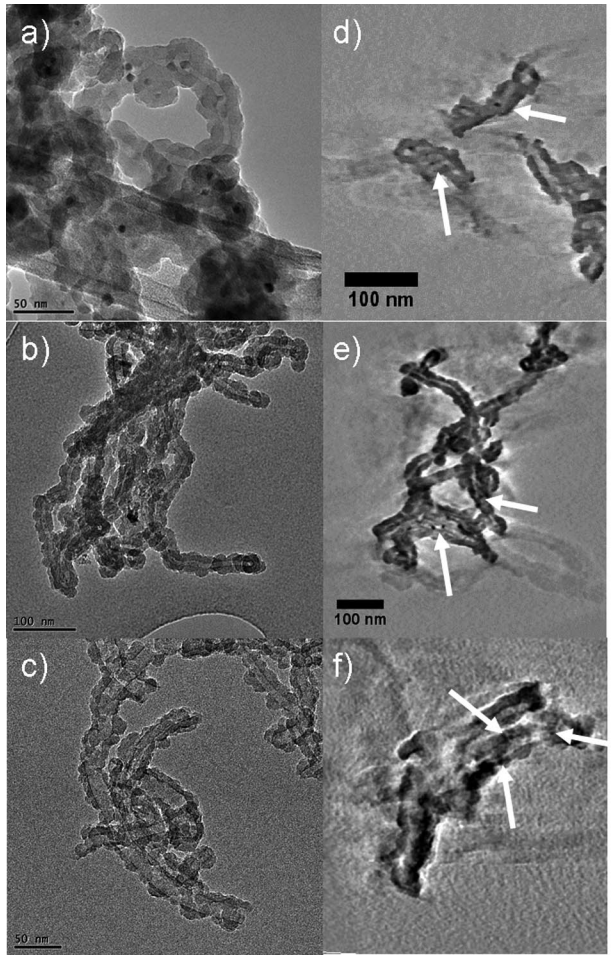

Figure 3. Cryo-TEM micrographs (–100 °C) of (a) Ru1@SiO_2NT, (b) Ru2@SiO_2NT, and (c) Ru3@SiO_2NT and typical slices through the reconstructed volumes obtained by cryo-TEM tomography on some representative agglomerates of (d) Ru1@SiO_2NT, (e) Ru2@SiO_2NT, and (f) Ru3@SiO_2NT.

Finally, to evaluate the accessibility of the confined Ru nanoparticles, we investigated their catalytic activity in the hydrogenation of cinnamaldehyde (20 bar H_2, 100 °C). All the confined samples showed high activity, turnover frequencies ranging between 175 and 200 h^{-1}, and selectivity values of approximately 45% for hydrocinnamyl alcohol, 40% for hydrocinnamaldehyde, and 15% for cinnamyl alcohol.

Conclusions

In summary, we have demonstrated a useful and effective method for the ultraselective confinement of ruthenium nanoparticles in silica nanotubes. The key to a successful coating consists in using Ru/CNTs as a template. We believe that this approach can be extended to many metal nanoparticles and will provide a useful tool for the research community whose interests involve confined metal or metal oxide nanoparticles.

Experimental Section

CNT Oxidation: Multiwalled carbon nanotubes (90% purity) were supplied from the same batch by Arkema, France, under the trademark Graphistrength®. The as-received CNTs were purified with a mixture of concentrated H_2SO_4/water (1:1) at 140 °C for 3 h to remove any residual metal catalyst. Then, the purified multiwalled CNTs (2 g) were suspended in concentrated nitric acid (65%, 80 mL) and heated at reflux at 140 °C for 3 h. After cooling, the CNTs were filtered, washed with distilled water until neutralization of the filtrate, and dried in air at 110 °C for 2 d.

Preparation of Ru/CNT: Three different ruthenium precursors were used and dissolved in appropriate solvents with a concentration calculated so as to give a theoretical value of 3 wt.-% Ru: $[Ru_3(CO)_{12}]$ (Ru1) in acetone, $RuCl_3$ (Ru2) in 2-propanol, and [Ru(cod)(cot)] (Ru3) in heptane. To prepare the catalysts from $[Ru_3(CO)_{12}]$ and $RuCl_3$, oxidized CNTs (200 mg) were dispersed in a solution of the precursor (20 mL) by ultrasonication for 20 min. After ultrasonic treatment, the mixture was stirred at room temperature until the solvent had evaporated and then dried overnight at 110 °C. For [Ru(cod)(cot)], the catalysts were prepared in a glove box by impregnation: The oxidized CNTs (100 mg) were immersed into a heptane solution (50 mL) of [Ru(cod)(cot)] and heated at reflux at 70 °C for 24 h under an atmosphere of argon. After cooling, the solid was filtered and dried overnight at 110 °C. For all of the prepared catalysts, the dried solids were reduced at 300 °C for 2 h in a furnace under flowing H_2/Ar (10% H_2 v/v) to transform the ruthenium precursor into the metal.

Preparation of SiO_2NT: The oxidized CNTs (50 mg) and a mixture of ethanol (250 mL) and ammonium hydroxide (8 mL) were charged into a 500 mL flask and mixed by ultrasonication for 30 min and stirring for 15 min. After dispersion, TEOS (6 mL) was injected quickly into the flask, and the solution was vigorously stirred at room temperature for 24 h. Upon completion of the reaction, the composite was washed with ethanol to remove secondary silica particles and dried overnight at 110 °C. Finally, SiO_2NTs were prepared by calcination of the silica-coated CNTs at 650 °C for 2 h in air.

Preparation of Ru@SiO_2NT

In Situ Method: Ru*x*/CNT (50 mg) and a mixture of ethanol (250 mL) and ammonium hydroxide (8 mL) were charged into a 500 mL flask and mixed by ultrasonication for 30 min and stirring for 15 min. After dispersion, TEOS (6 mL) was injected quickly into the flask, and the solution was vigorously stirred at room temperature for 24 h. Upon completion of the reaction,, the composite was washed with ethanol, dried overnight at 110 °C, and then calcined at 650 °C for 2 h in air. Finally, the Ru*x*@SiO_2NTs were reduced at 300 °C for 2 h in a furnace under flowing H_2/Ar (10% H_2 v/v).

Ex Situ Method: SiO_2NT (50 mg) were dispersed in a solution of $[Ru_3(CO)_{12}]$ in acetone (5 mL, to achieve a theoretical value of 3 wt.-% Ru) by ultrasonication for 30 min. After ultrasonic treatment, the mixture was stirred at room temperature until the acetone had evaporated. The $[Ru_3(CO)_{12}]$@NTs samples were dried overnight and then reduced at 300 °C for 2 h in a flow of H_2/Ar.

Characterization: Thermogravimetric analysis (TGA) in air was conducted with a Setaram apparatus by using a temperature program of 25–1000 °C with a heating rate of 10 °C min^{-1}. X-ray diffraction (XRD) was performed with a Panalytical MPD Pro powder diffractometer at room temperature by using Cu-K_α radiation (λ = 0.15418 nm). TEM images and electron tomography data were acquired with a JEOL 2100F transmission electron microscope with a field emission gun operating at 200 kV equipped with a probe corrector and a GATAN Tridiem energy filter. Before observation, the powders were dispersed in ethanol by sonication, and several droplets were deposited onto a cooper grid covered by a carbon holey membrane. For the tomographic experiment, the tilt series was acquired by tilting the specimen over a range of ±60°; an image was recorded every 2° in the Saxton mode. The acquisitions were carried out at low temperature (about 100 K) to reduce irradiation damage in the organic part of the layer during the total duration of the acquisition process (1 h). The images of the tilt series were initially aligned by using a cross-correlation algorithm. Refinement of this initial alignment was obtained by considering the centers of several Ru nanoparticles as fiducial markers. The volume reconstructions were computed by using iterative algorithms based on algebraic reconstruction techniques implemented in the TOMOJ software, with a number of 20 iterations. Visualization and quantitative analysis of the final volumes were done by using ImageJ software.

Supporting Information (see footnote on the first page of this article): TGA curves, TEM micrographs, and XRD diagrams.

Acknowledgments

T. T. N. thanks the Université des Sciences et Technologie d'Hanoï (USTH) Consortium and the Ministry of Education and Training of Vietnam for her PhD grant. The authors acknowledge financial support from the French Centre National de la Recherche Scientifique (CNRS) (FR3507) and the Commissariat à l'Énergie Atomique et aux Énergies Alternatives – Microscopie Electronique et Sonde Atomique (CEA METSA) network.

[1] a) P. Serp, E. Castillejos, *ChemCatChem* **2010**, *2*, 41–47; b) X. Pan, X. Bao, *Acc. Chem. Res.* **2011**, *44*, 553–562; c) D. M. Vriezema, M. Comellas Aragonès, J. A. A. W. Elemans, J. J. L. M. Cornelissen, A. E. Rowan, R. J. M. Nolte, *Chem. Rev.* **2005**, *105*, 1445–1490; d) A. Ostafin, K. Landfester (Eds.), *Nanoreactor Engineering for Life Sciences and Medicine*, Artech House, Norwood, MA, **2009**; e) C. Edlinger, X. Zhang, O. Fischer-Onaca, C. G. Palivan, *Encyclopedia of Polymer Science and Technology*, Wiley, New York, **2002**.

[2] a) F. Goettmann, C. Sanchez, *J. Mater. Chem.* **2007**, *17*, 24–30; b) A. Noy, H. G. Park, F. Fornasiero, J. K. Holt, C. P. Grigoropoulos, O. Bakajin, *Nano Today* **2007**, *2*, 22–29; c) A. Mataz, B. M. Gregory, *J. Phys. Condens. Matter* **2005**, *17*, R461; d) P. E. de Jongh, M. Allendorf, J. J. Vajo, C. Zlotea, *MRS Bull.* **2013**, *38*, 488–494.

[3] a) V. Ramamurthy, *J. Photochem. Photobiol. C: Photochem. Rev.* **2000**, *1*, 145–166; b) G. Sastre, A. Corma, *J. Mol. Catal. A* **2009**, *305*, 3–7; c) R. Gounder, E. Iglesia, *Chem. Commun.* **2013**, *49*, 3491–3509.

[4] G. Buntkowsky, H. Breitzke, A. Adamczyk, F. Roelofs, T. Emmler, E. Gedat, B. Grunberg, Y. Xu, H.-H. Limbach, I. Shenderovich, A. Vyalikh, G. Findenegg, *Phys. Chem. Chem. Phys.* **2007**, *9*, 4843–4853.
[5] X. Pan, X. Bao, *Nanomaterials in Catalysis*, Wiley-VCH, Weinheim, **2013**, pp. 415–441.
[6] a) J. H. Jung, M. Park, S. Shinkai, *Chem. Soc. Rev.* **2010**, *39*, 4286–4302; b) J. A. García-Calzón, M. E. Díaz-García, *TrAC Trends Anal. Chem.* **2012**, *35*, 27–38; c) Y. Lin, Y. Qiao, Y. Wang, Y. Yan, J. Huang, *J. Mater. Chem.* **2012**, *22*, 18314–18320.
[7] J.-P. Tessonnier, O. Ersen, G. Weinberg, C. Pham-Huu, D. S. Su, R. Schlögl, *ACS Nano* **2009**, *3*, 2081–2089.
[8] Q. Fu, W. Gisela, D.-s. Su, *New Carbon Mater.* **2008**, *23*, 17–20.
[9] E. Castillejos, P.-J. Debouttière, L. Roiban, A. Solhy, V. Martinez, Y. Kihn, O. Ersen, K. Philippot, B. Chaudret, P. Serp, *Angew. Chem.* **2009**, *121*, 2567–2571; *Angew. Chem. Int. Ed.* **2009**, *48*, 2529–2533.
[10] S. Takenaka, H. Matsumori, T. Arike, H. Matsune, M. Kishida, *Top. Catal.* **2009**, *52*, 731–738.
[11] a) S. Takenaka, H. Matsumori, K. Nakagawa, H. Matsune, E. Tanabe, M. Kishida, *J. Phys. Chem. C* **2007**, *111*, 15133–15136; b) Z. Sun, H. Zhang, Y. Zhao, C. Huang, R. Tao, Z. Liu, Z. Wu, *Langmuir* **2011**, *27*, 6244–6251.
[12] S. Guo, S. Dong, E. Wang, *J. Phys. Chem. C* **2008**, *112*, 2389–2393.
[13] H.-q. Tang, J.-l. Li, *J. Fuel Chem. Technol.* **2011**, *39*, 615–620.
[14] H. Tang, K. Liew, J. Li, *Sci. China Chem.* **2012**, *55*, 145–150.
[15] I. Gerber, M. Oubenali, R. Bacsa, J. Durand, A. Gonçalves, M. F. R. Pereira, F. Jolibois, L. Perrin, R. Poteau, P. Serp, *Chem. Eur. J.* **2011**, *17*, 11467–11477.
[16] M. Kim, J. Hong, J. Lee, C. K. Hong, S. E. Shim, *J. Colloid Interface Sci.* **2008**, *322*, 321–326.
[17] Z.-H. Yin, X. Liu, Z.-X. Su, *Bull. Mater. Sci.* **2010**, *33*, 351–355.
[18] Q. Liao, Y. Wang, Y. Gao, H. Li, *Curr. Nanosci.* **2010**, *6*, 243–248.
[19] Y. Yang, S. Qiu, W. Cui, Q. Zhao, X. Cheng, R. Li, X. Xie, Y.-W. Mai, *J. Mater. Sci.* **2009**, *44*, 4539–4545.
[20] E. Asedegbega-Nieto, B. Bachiller-Baeza, D. G. Kuvshinov, F. R. García-García, E. Chukanov, G. G. Kuvshinov, A. Guerrero-Ruiz, I. Rodríguez-Ramos, *Carbon* **2008**, *46*, 1046–1052.
[21] C. Mateo-Mateo, C. Vázquez-Vázquez, M. Pérez-Lorenzo, V. Salgueiriño, M. A. Correa-Duarte, *J. Nanomater.* **2012**, 404159.
[22] G. Battaglin, A. Carnera, G. Lodi, E. Giorgi, A. Daghetti, S. Trasatti, *J. Chem. Soc. Faraday Trans. 1* **1984**, *80*, 913–917.
[23] H. Over, M. Muhler, *Prog. Surf. Sci.* **2003**, *72*, 3–17.
[24] T. Koerts, J. H. M. C. van Wolput, A. M. de Jong, J. W. Niemantsverdriet, R. A. van Santen, *Appl. Catal. A* **1994**, *115*, 315–326.
[25] Y. Li, L. Yao, Y. Song, S. Liu, J. Zhao, W. Ji, C.-T. Au, *Chem. Commun.* **2010**, *46*, 5298–5300.

Received: July 16, 2013
Published Online: September 23, 2013

